Optimizing Polymer Affinity Agent Properties for Surface-enhanced Raman Scattering Detection of Aflatoxin B1

Victoria M. Szlag^{†‡}, Rebeca S. Rodriguez^{†‡}, Seyoung Jung["], Marc R. Bourgeois[§], Samuel Bryson[†], Anatolii Purchel[†], George Schatz[§], Christy L. Haynes*[†], Theresa M. Reineke*[†]

†Department of Chemistry and *Department of Chemical Engineering and Materials Science,

University of Minnesota, Minneapolis, Minnesota 55455, United States

§Department of Chemistry and International Institute for Nanotechnology, Northwestern University, 2145 Sheridan Road, Evanston, Illinois 60208 United States

KEYWORDS: polymer affinity agent, surface-enhanced raman spectroscopy, aflatoxin b1, ITC, DFT

ABSTRACT: A series of poly(N-acryloyl glycinamide) (pNAGA) were synthesized and studied as capture agents for surface-enhanced Raman scattering (SERS) detection of aflatoxin B1 (AFB1), a highly carcinogenic food-borne toxin. Four molecular weights of pNAGA were polymerized by reversible addition fragmentation chain transfer (RAFT) polymerization to study

the dependence of affinity agent efficacy on chain length for this AFB1 sensing platform. The polymer lengths studied, pNAGA14 (2.0 kDa), pNAGA22 (3.1 kDa), pNAGA30 (4.1 kDa), and pNAGA₃₈ (5.1 kDa), had low dispersity (~ 1.1) and functional groups that allow easy attachment to plasmonic substrates. Isothermal titration calorimetry (ITC) was used to verify the sign and magnitude of the enthalpic effects involved in polymer-AFB1 interactions in solution and understand the effects of pNAGA chain length on AFB1 noncovalent binding; pNAGA-AFB1 interactions were found to be exothermic, and longer pNAGA chains generally resulted in smaller enthalpy decreases per repeat unit. With pNAGA22 being thermodynamically the strongest agent, AFB1 affinity is suspected to be determined by a balance between the configurational restrictions in pNAGA chains and the enthalpic advantage of binding AFB1. SERS spectral changes observed following AFB1 exposure were used to evaluate the influence of polymer molecular weight (2.0 - 5.2 kDa), attachment chemistry (thiol vs. trithiocarbonate), and order of addition (pre- vs. post- functionalization of the substrate) on the sensitivity of AFB1 detection. The method by which target, polymer affinity agent, and signal transduction mechanism are combined was found to have significant impacts on the sensitivity. The best polymer chain length (pNAGA₂₂), anchoring chemistry (thiol), and polymer/toxin assembly scheme (in-solution) allowed detection of 10 ppb AFB1 in water (below the FDA regulatory limit of 20 ppb), a hundred-fold improvement over SERS sensing without the pNAGA affinity agent.

INTRODUCTION:

Polymers combined with analytical signal transduction mechanisms have the potential to create inexpensive, versatile sensing platforms. Literature precedent demonstrates that polymers in sensing technologies can produce sensitive, inexpensive, and robust devices. In the majority of published work, polymers are used as sensor substrates;^{2,3} however, given their benefits such as easy chemical modification and inexpensive synthesis, polymers are attractive subjects to develop as affinity (analyte-capturing) agents, as well.⁴ As affinity agents, polymers provide several handles for optimizing sensor performance. They can be synthesized with desired analyte selectivity, using molecular hypotheses of target/polymer interactions. ⁵ The end groups and repeat units of the polymer can be chemically modified to enable surface attachment and adjust chain properties (e.g. charge, polarity), respectively. ^{6–8} Using controlled polymerization methods, polymer chain lengths can easily be tuned to change the number of binding sites or surface assembly on a platform. The use of polymer affinity agents can also provide other benefits to a sensor platform; for example, synthetic polymers are typically more thermally stable¹⁰ compared to biologically-derived agents.¹¹ Thus, platforms using polymer affinity agents have a long shelf-life and are suitable for use in resource-limited settings, e.g., no access to refrigeration. Moreover, polymer affinity agents demonstrate less target specificity, and thus, a single polymer may be used as an affinity agent for multiple targets. 12-16 Multi-target affinity agents can increase the device versatility and decrease the cost, given the use of a detection system suited for the multiple targets. Surface-enhanced Raman spectroscopy (SERS) is such a sensing technique, enabling multiplex detection, though often requiring the use of an affinity agent for best performance.

The popularity of SERS^{17–19} as a signal transduction mechanism stems from the analytical advantages of this technique: analyte-unique vibrational signatures, compatibility with

aqueous matrices, and low limits of detection. The unique analyte signature produced²⁰ is due to the Raman scattering of light by the molecular bonds of the analyte.²¹ The detection of analytes in aqueous environments, ¹⁹ such as biological matrices, is possible due to the poor inherent Raman scattering cross-section of water. 22 When an analyte is confined near a plasmonic metal surface, low concentrations of this analyte can be detected.²³ These surfaces with a localized surface plasmon resonance (LSPR), typically have nanoscale roughness which produces short range electromagnetic (EM) fields²⁴ and leads to large (10⁴-10¹⁴) Raman signal enhancement.²⁵ Many SERS detection platforms rely on affinity agents to capture and concentrate analytes in this enhancing electromagnetic field. Affinity agents can also add an element of specificity and prevent surface fouling whilst sensing in complex matrices. Bio-based affinity agents such as antibodies^{26–28} and aptamers^{29–33} are commonly used. As previously mentioned, polymers are a viable alternative to these traditional SERS affinity agents. Although the use of linear, singlepoint-attachment polymers as SERS affinity agents is not common, previous work has demonstrated the utility of such a platform for sensing a protein toxin in food matrices.³⁴ In that work, the polymer affinity agent was designed with pendant saccharides to capture the toxin by exploiting a natural binding pocket present on the protein.

Toxins of biological origin come from many sources and pose a serious threat to human health. In addition to macromolecular toxins such as proteins, small molecule biotoxins such as those produced by algae in drinking water resources³⁵ and fungi that contaminate food require constant monitoring to ensure safety of ingestion.³⁶ Of the toxins produced by fungi (mycotoxins), aflatoxin B1 (AFB1) is the most toxic and carcinogenic,³⁷ and is thus the most heavily regulated worldwide. The US FDA regulatory limit for AFB1 in food is 20 ppb.³⁸ Monitoring techniques used commercially are enzyme linked immunosorbent assay (ELISA),

monoclonal antibody affinity chromatography, lateral flow strips, fluorescence technology, and high performance liquid chromatography (HPLC).³⁹ Academically, SERS detection of aflatoxins has been pursued for its ability to output characteristic spectra of the target, which could enable multiplex detection in the presence of other mycotoxins, theoretically without compromising sensitivity, specificity, or speed. SERS of AFB1 without affinity agents either had sufficient LODs (13-36 ppb) but poor reproducibility due to substrate problems⁴⁰ or excellent reproducibility at LODs (15 ppm) above the regulatory limit.⁴¹ AFB1 SERS sensors that have used affinity agents that are either aptamers (LOD 0.03 ppb AFB1)³² or antibodies (LOD 0.10 ppb).²⁷ However, both examples are extrinsic SERS sensors, which does not measure the vibrational modes of the target directly, but instead monitors a SERS reporter. Such extrinsic sensing loses the benefit of SERS as a label-free technique, inherently capable of multiplex detection based on specific vibrational modes of AFB1 and other analytes. Therefore, to enable a generalizable platform, the efficacy of polymer affinity agents must be tested for small molecule analytes.

In this work, we synthesize and examine the use of new polymer affinity agents employing N-acryloyl glycinamide (NAGA) to directly detect AFB1 via a SERS detection platform. This new affinity agent is combined with the relatively inexpensive, simple, and tunable SERS substrate that has been previously used for sensing applications:^{29,34,42–44} film over nanosphere (FON) wafers fabricated by nanosphere lithography.⁴⁵ Inspired by the previous work by Piletska *et al.*, the NAGA repeat unit was designed to function as the AFB1 binding site. The hypothesized pNAGA/AFB1 noncovalent binding was inspired by the interactions reported between N,N,-methylene bisacrylamide (MBAA) and AFB1.⁴⁶ NAGA was used to preserve the functional groups responsible for AFB1 affinity, but allow the controlled radical polymerization

of linear polymers. Herein, a polymer affinity agent/small molecule analyte system has been studied. We investigated how SERS detection of the analyte was affected by polymer chain length, endgroup (promotes SERS substrate attachment), and the order of polymer chain addition to the detection platform: pre-functionalized to the gold surface prior to AFB1 exposure or postfunctionalized to the gold surface after AFB1 exposure. Four degrees of polymerization (pNAGA₁₄, pNAGA₂₂, pNAGA₃₀ and pNAGA₃₈) were synthesized, by reversible additionfragmentation chain transfer (RAFT) polymerization, to enable the systematic study of chain length on affinity agent performance. It was hypothesized that a mid-range molecular weight of pNAGA would perform best by maximizing the number of binding sites (repeat units) without being so large as to coil and form competing intramolecular H-bonds, as previously seen with other long-chain polymers binding AFB1 in solution.⁴⁷ The RAFT chain transfer agent (CTA) also provides a functional handle shown to bind to gold surfaces important to SERS substrates. 48-⁵¹ This trithiocarbonate end group can be used to directly functionalize gold SERS substrates with the polymer or be reduced to a thiol, which also has a high affinity for linkage to a gold surface.⁵² In this work, the best performing pNAGA molecular weight was used to evaluate both trithiocarbonate and thiol end groups (Figure 1, panels B and C) in affinity agents. It was hypothesized that the thiol-terminated polymer would perform better than the trithiocarbonate due to fewer intrinsic S-C Raman vibrations, which can mask AFB1 vibrational modes. Lastly, the order of polymer affinity agent exposure to the gold surface was examined in detail. As shown in Figure 1, panels B and C denote pre-functionalization of the gold with the polymer prior to AFB1 exposure, and panels D and E denote post-functionalization of gold after polymer exposure to AFB1. We hypothesized that the chains exposed to AFB1 in-solution to be more accessible to the toxin and thus can bind more AFB1 and generate better SERS signal. Overall,

this is an interesting and relevant system from which to explore the utility of polymer affinity agents for sensing platforms, and the impact of chain length, attachment chemistry, and order of affinity agent/target exposure on sensor performance.

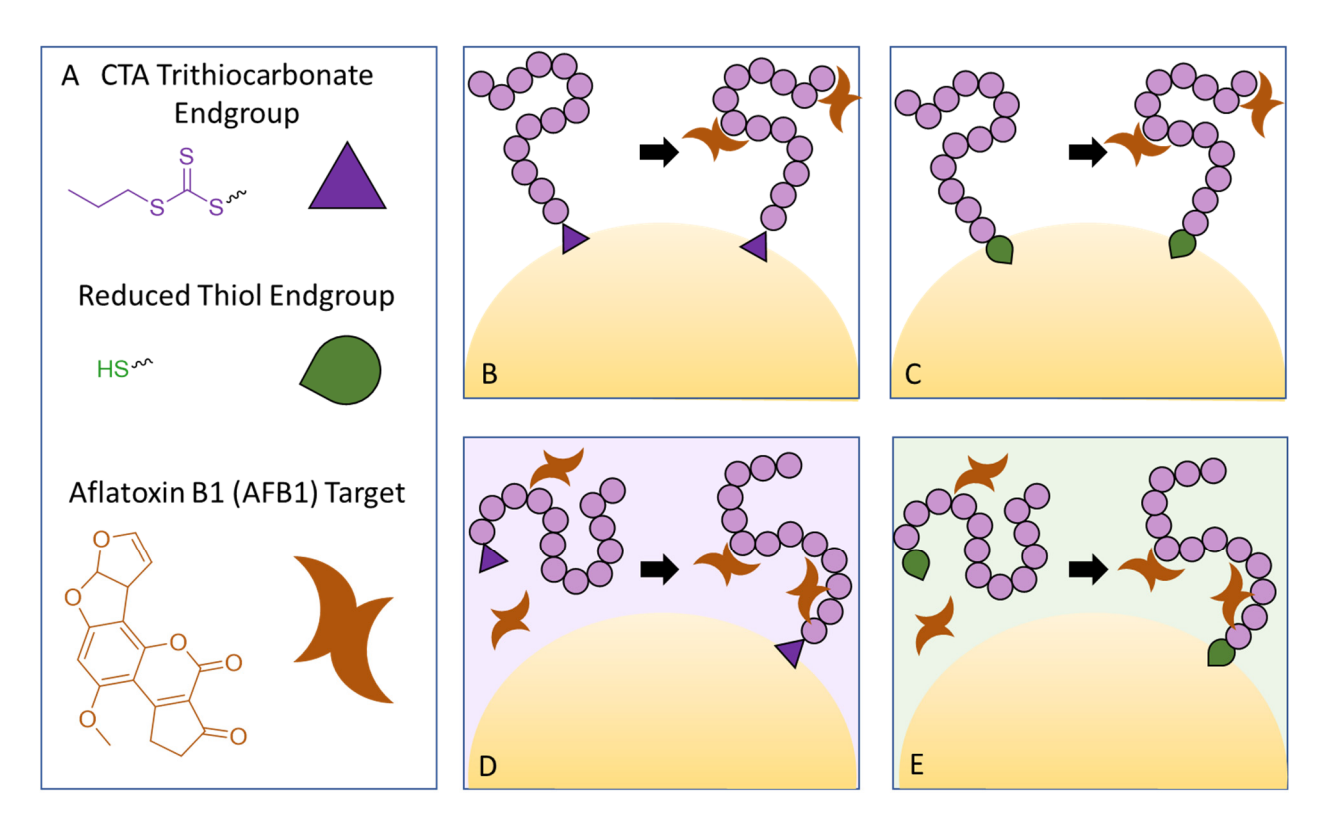


Figure 1. Illustrative representation of the studies completed in this work: both the role of the polymer-gold attachment chemistry (trithiocarbonate versus thiol) and order of polymer affinity agent functionalization (pre- or post-functionalized) on the gold surface has been examined in detail. B and D denote trithiocarbonate (purple triangle) linkage versus C and E, which denote thiol (green teardrop) linkage, and the order of polymer affinity agent exposure to the gold surface: B and C denote pre-functionalization of the gold with the polymer prior to AFB1 (orange crescents) exposure, and D and E denote post-functionalization of gold after polymer exposure to AFB1.

MATERIALS AND METHODS:

Materials

Chemicals were used as purchased unless specified otherwise. Potassium carbonate, anhydrous (Certified ACS) was purchased from Fisher Chemical. Tris(2-carboxyethyl)phosphine hydrochloride (TCEP, ≥98%), N-propylamine (≥99%), glycinamide hydrochloride (≥98%), aflatoxin B1 from *Aspergillus flavus* (AFB1, ≥98%), and 4,4′-azobis(4-cyanovaleric acid) (V501, ≥75%), were purchased from Sigma-Aldrich. The chain transfer agent (CTA) 4-cyano-4-(propylsulfanylthiocarbonyl)sulfanylpentanoic acid (CPP) was synthesized as previously reported.⁵³ Silica spheres, 590-nm-diameter (10% solids), were purchased from Bangs Laboratories, Inc (Fishers, IN). High purity gold (99.999%) Au) was purchased from Kurt J Lesker, (Clairton, PA).

Synthesis of N-acryloyl glycinamide (NAGA) Monomer

The monomer N-acryloyl glycinamide was prepared as previously reported by Seuring et al, 54 omitting the final purification step of recrystallization. Briefly, 4.59 g glycinamide hydrochloride (41.4 mmol) and 11.3 g potassium carbonate (81.3 mmol) were dissolved in 25 mL water and cooled in an ice bath. Under rapid stirring (300 rpm), 63.3 mL of 0.68 M acryloyl chloride in diethyl ether solution was added over 30 minutes. The flask was further stirred at room temperature for 2 hrs. Safety note: pressure can build in the reaction flask, and a venting mechanism is recommended. Removal of the diethyl ether, freeze drying of the aqueous layer, extraction of the crude solid with acetone, and purification of the crude extraction solution by column chromatography was performed as previously reported. Yield of monomer after the column was 3.0 g (57%). DSC (rate of heating = 10 K/min; Figure S1): $T_m = 137$ °C. H NMR

(500 MHz, DMSO_d; Figure S2): δ = 3.73 (s, 2H, N- CH₂-CONH₂), 5.61 (dd, 1H, CH), 6.11 (dd, 1H, CH₂), 6.31 (dd, 1H, CH₂), 7.03 (s, 1H, NH₂), 7.36 (s, 1H, NH₂), 8.27 (s, 1H, NH).

Synthesis of poly(N-acryloyl glycinamide) (pNAGA) Polymers

The four molecular weights of pNAGA polymer were prepared by RAFT polymerization, similar to previously reported work.^{34,47,55} The polymerizations were performed in dimethyl sulfoxide (DMSO). For each synthesized molecular weight, molar concentrations and volumes of the monomer NAGA, initiator 4'-azobis(4-cyanovaleric acid), and chain transfer agent (CTA) 4cyano-4-(propylsulfanylthiocarbonyl) sulfanylpentanoic acid added can be found in Table S1 in the Supporting Information. A typical polymerization was carried out as follows: the monomer, initiator, and CTA were dissolved independently in DMSO, combined in the reaction flask and degassed by three cycles of freeze, pump, thaw. The reactions were then polymerized for 16 h at 75 °C. Polymer samples were dialyzed against 700 mL water for 18 h followed by two 700 mL water exchanges for 3 h each. The samples were lyophilized and characterized by sized exclusion chromatography (SEC) and NMR. For SEC (Agilent 1260 Infinity Quaternary LC System with Eprogen columns at 40 °C [CATSEC1000 (7 μ m, 50 × 4.6), CATSEC100 (5 μ m, 250×4.6), CATSEC300 (5 µm, 250×4.6), and CATSEC1000 (7 µm, 250×4.6)]; Wyatt HELEOS II light scattering detector ($\lambda = 662$ nm) at 30 °C, and an Optilab rEX refractometer (λ = 658 nm)); 0.1 M Na2SO4 in 1.0 v% acidic acid mobile phase; dn/dc = 0.185, traces can be seen Figure S3. ¹H NMR (500 MHz, DMSO_d; Figure S4): $\delta = 0.95$ (s, 3H, -CH₃ end group), 1.24-2.07 (m, 3H, CH-CH₂ backbone), 3.57-4.05 (m, 2H, CH₂), 7.08-8.68 (m, 3H, NH & NH₂).

Reduction of pNAGA Trithiocarbonate End Groups to Thiols

Reduction of the endgroups to thiols was carried out following a protocol by Zhou *et al.*⁵² pNAGA₂₂ was dissolved in 10 mL Mili-Q water (2.2 mM) and purged under nitrogen gas for 30 minutes. *N*-propylamine (2 mmol) and tris(2-carboxyethyl) phosphine HCl (TCEP) (0.04 mmol) were dissolved into the polymer solution and stirred overnight to ensure full conversion. Modification was confirmed via observation of SERS vibrational changes (see Figure S9 in Supporting Information), detailed in Results and Discussion.

Isothermal Titration Calorimetry (ITC)

ITC of the pNAGA-AFB1 systems was performed using a MicroCal PEAQ-ITC Automated (Malvern Instruments, Westborough, MA) at 25 °C, similar to previously published work.⁴⁷ All solution transfers and injections were automated. Cleaning of the cell and injection syringe with subsequent 20% Contrad 70 detergent, water, and methanol preceded all experimental runs. Polymer solutions were made at a concentration of 4.0 mM NAGA repeat units in 22% DMSO, 16% methanol, 62% acetate buffer (pH 5) and transferred to the injection syringe. The DMSO/MeOH/acetate mixture was used to create 0.26 mM AFB1 solutions, or as a blank solvent for background titrations, and was transferred to the sample cell. The titrations consisted of 1.5 µL injections of pNAGA solution (in syringe) into AFB1 solution for blank solvent (in sample cell) every 150 s. Raw ITC data (as seen in the left two columns of Figure S5) is measured as heat flow rate as a function of time, displaying a peak with each injection. Final ITC results, depicting total heat absorption at each injection versus polymer repeat unit (RU)/toxin ratio, are the integration of the raw heat flow data with respect to time. The enthalpy change exclusively from AFB1-polymer interactions (ΔH_{int}) was determined by subtracting (point-by-point) the enthalpy change measured in the background titration of polymer injected into solvent (ΔH_{bgd}) from that in the main titration of polymer injected into AFB1 (ΔH_{main}).

SERS measurements were performed using a Snowy Range Instruments SnRI ORS system with 785 nm laser, 9 mW incident power, and 10 sec integration time. The SERS substrates used, gold film over nanospheres (FON) with a localized surface plasmon resonance maximum between 720-820 nm as measured by a fiber optic probe (Ocean Optics, Dunedin, Florida) with a flat gold film as the reflective standard, were fabricated as previously reported.

34,43,47 Non-resonant Raman spectra of the monomer NAGA under 785 nm excitation were calculated with the Amsterdam Density Functional (ADF) computational chemistry package⁵⁶, using Becke-Perdew (BP86)⁵⁷ generalized gradient approximation (GGA), and B3LYP⁵⁸ hybrid exchange-correlation functionals, as previously reported.⁴⁷

In this work, two types of SERS experiments were conducted: post-polymer attachment AFB1 exposure and pre-polymer attachment AFB1 exposure. In the former, pNAGA was first attached to the gold FON by incubating the FON in a 1.0 mM pNAGA solution for 18 h. Subsequently, the pNAGA-functionalized FONs were exposed to a known concentration of AFB1 dissolved in 4:6 MeOH/water for 6 h. The FONs were rinsed with 1 mL of water, dried, and measured by SERS.

In the pre-polymer attachment AFB1 exposure, a 1.0 mM pNAGA solution was incubated with a known concentration of AFB1 dissolved in 4:6 MeOH/water for 6 h. Bare FONs were then exposed to the pNAGA/AFB1 solution for 18 h, rinsed with 1 mL of water, air dried, and measured by SERS. SERS spectra were measured on 5 spots per FON, and three FON replicates were performed per experiment. The five SERS spectra from each FON were averaged, baselined (Origin 9.1, eleven anchor points, found using the first and second derivative

with Savitzky-Golay smoothing, and connected by B-spline interpolation, utilizing the same number of points as the input spectrum), and normalized by the incident power and integration time. Peak height and ratios that appeared to be AFB1 concentration-dependent were statistically analyzed by one-way ANOVA with a Tukey post-hoc using the program R.⁵⁹

RESULTS AND DISCUSSION:

Synthesis of pNAGA Polymers for AFB1 Binding

Synthesis of the NAGA monomer followed a procedure that minimized acrylic acid impurities, a common side product in the reaction of acryloyl chloride and glycinamide hydrochloride, due to the importance of the presence of pendent amide for interaction with the biological toxin AFB1. These byproducts cannot be observed by NMR (Figure S2 in Supporting Information) and must be detected at <1% wt by DSC. The T_m of the synthesized monomer is 136 °C (Figure S1 in Supporting Information) and is lower than that reported for ultrapure NAGA samples (143 °C, <0.01 % acrylate) but higher than reported samples with 0.12% acrylic acid (132 °C), indicating an acrylic acid content <0.12%.⁵⁴ As the thermal properties, which are disrupted by such low amounts of acrylate, are not the focus of this work, the monomer was deemed sufficiently pure for polymerization. Using the chain transfer agent (CTA) 4-cyano-4-(propylsulfanylthiocarbonyl)sulfanylpentanoic acid (CPP), four molecular weights of pNAGA were polymerized by RAFT (Table 1). In addition to providing useful sulfur moieties for later gold attachment, ^{48–50} the use of RAFT polymerizations resulted in low dispersities which enable the study of size-dependent effects between polymer populations. The targeted chain lengths spanned from oligomeric to moderately sized polymers to enable the study of chain lengthdependent trends in AFB1 interactions, exposed either in solution or on gold SERS substrates.

Based on previous work with amine and alcohol pendent polymers, it was hypothesized that, in dilute conditions, short-mid chain lengths would demonstrate higher affinity per repeat unit in solution due to low intramolecular interactions and low chain coiling, resulting in higher availability of each repeat unit. We also hypothesized that for the application of SERS, midlength chains would outperform short chains due to the denser packing of short chains on the gold SERS surface, limiting the access of AFB1 to the enhancing electromagnetic field at the SERS substrate surface.

A NAGA Monomer Synthesis

B NAGA RAFT Polymerization

N-acryloyl glycinamide

Poly(*N*-acryloyl glycinamide)

Scheme 1. (A) NAGA synthesis (B) RAFT polymerization of NAGA

pNAGA synthesized by RAFT polymerization provided the control necessary to create four molecular weights of targeted size and low dispersity. A family of molecular weights were synthesized and studied for the effect of chain length on interactions with AFB1 in solution by ITC and on a surface by SERS.

Table 1. Characterization of pNAGA polymers synthesized by RAFT, number of NAGA repeat units are denoted in name subscript; M_n, M_w, and D measured by SEC.

Polymer	M _n (kDa)	Mw (kDa)	Đ
pNAGA ₃₈	5.11	5.52	1.08
pNAGA ₃₀	4.08	4.53	1.12
pNAGA ₂₂	3.12	3.40	1.09
pNAGA ₁₄	2.01	2.25	1.12

In-Solution Interactions of pNAGA with AFB1

The in-solution interaction of pNAGA and AFB1 was studied by measuring the enthalpy change in the system when pNAGA was titrated into a solution of AFB1, using ITC. ITC has long been used to quantify protein/ligand interactions, and has more recently been used to study polymer systems, such as the interactions between polycations and DNA. ⁶⁰ In our system, we controlled the concentration of repeat units, which are the hypothesized AFB1 binding sites, to be the same for each polymer solution. If enhanced binding effects were observed due to more binding sites localized to a single chain (i.e. longer chains), the enthalpy change per repeat unit would be greater at a given RU/toxin ratio, compared that with a shorter chain.

Dilute, buffered pNAGA solution ([RU] = 4.0 mM) was titrated into AFB1 solution (0.26 mM) prepared with the same solvent mixture, and heat release was observed for all polymers (Figure S5 in Supporting Information). Note that heat was release during polymer dilution (into blank solvent) to a much smaller extent. Subtracting ΔH_{bgd} from ΔH_{main} , it was found that

pNAGA-AFB1 interactions are exothermic, indicating enthalpically favorable noncovalent interactions between pNAGA and AFB1,⁶¹ as expected from the simulations of a similar bisamide binding AFB1.⁴⁶

The instantaneous enthalpy change as a function of RU/toxin molar ratio was plotted and compared between different chain lengths of pNAGA. Figure 2 compares the integrated, background-subtracted data. The absence of the classic sigmoidal shape precludes the typical binding model-based fitting of the data; however, important trends within the pNAGA series are still apparent. The shorter chain lengths of pNAGA₁₄ and pNAGA₂₂ showed larger magnitudes of binding enthalpy per repeat unit than their longer counterparts, pNAGA₃₀ and pNAGA₃₈. This is suspected to be due to entropic restrictions in pNAGA chain conformation and potential intramolecular interactions which may decrease the effective number of available "binding sites". A similar trend has previously been observed with comparable chain lengths of poly(2-hydroxyethyl methacrylate) (pHEMA), as well.⁴⁷

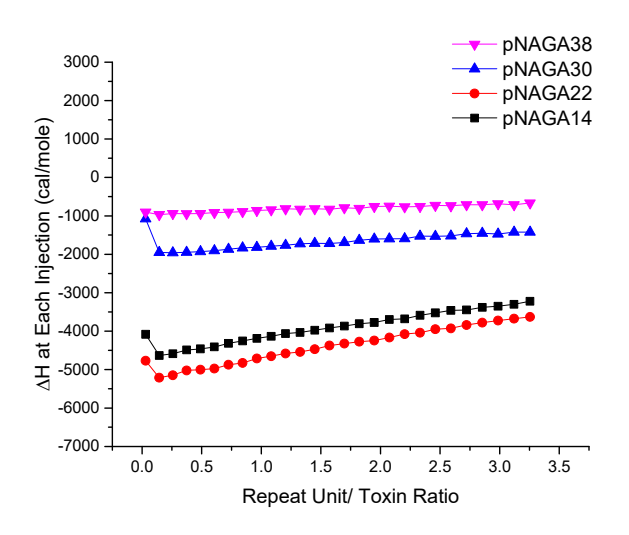


Figure 2. Integrated ITC profiles of pNAGA polymers (4.0 mM RU) titrated into 0.26 mM AFB. All titrations were performed in 22% DMSO, 16% methanol, 62% acetate buffer (pH 5).

SERS of pNAGA Polymers

To assist with the interpretation of experimental SERS spectra from pNAGA and pNAGA exposed to AFB1, the non-resonant Raman scattering spectrum of the monomer Nmethacryloyl glycinamide (NMAGA) was calculated using density functional theory. The calculated spectrum is used to rationalize the measured Raman frequencies and attribute them to specific vibrational modes within the molecule. Figure 3 shows the calculated spectrum of NMAGA plotted with a previously reported calculated spectrum of dipropyl carbonotrithioate (DPCTT), to represent the signal from the CPP anchor group. A full list of peak assignments, made visually, can be found in the Supporting Information (Table S2). Using this information, we identified peaks originating from vibrations of the primary amide: 611, 822, 1044, 1248, 1322, 1344, and 1561 cm⁻¹ shift. It was hypothesized that some, or all, of these vibrations may experience frequency shifts or changes in relative amplitude as pNAGA associates with AFB1 via hydrogen bonding. Vibrational modes from the CPP anchor group were not anticipated to change with AFB1 exposure. Strong vibrational modes from the anchoring group that did not overlap with modes from NMAGA, such as 516, 653, 959 and 1282 cm⁻¹ shift, were proposed as appropriate groups for spectral normalization.

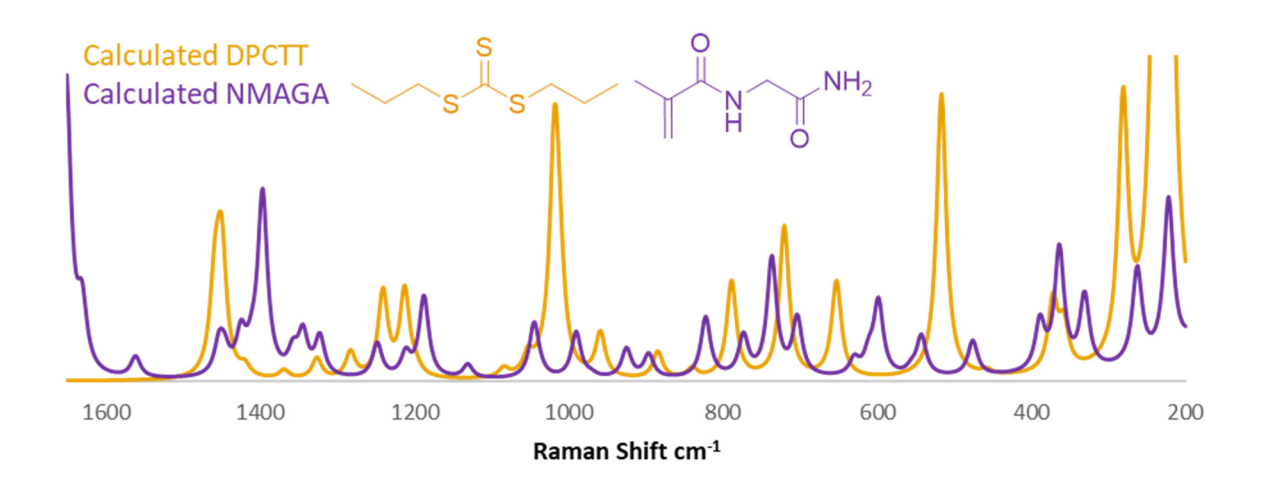


Figure 3. Calculated normal Raman spectrum of NMAGA plotted with calculated normal spectrum of DPCTT as shown by our previous work.⁴⁷

In addition to enabling predictions about spectral changes due to AFB1, the calculated normal Raman spectra assisted in the characterization of the polymer on the SERS substrate. Proximity and orientation of an affinity agent on a SERS surface can change the magnitude, and to a lesser extent, location of the vibrational bands, when comparing computed spectra to experimental spectra. Significant broadening of the pNAGA experimental spectra was observed relative to the computed monomer spectra, as expected due to the spectral averaging of the ensemble of real chain conformations relative to the SERS substrate. All four molecular weights of pNAGA demonstrated a pattern of vibration similar to those predicted (Figure 4). These spectra signify polymer attachment, even after rinsing, and sufficient surface coverage. The SERS of the four polymers gave further chemical information. With increasing chain length, relative peak magnitudes changed for several pNAGA and CPP vibrations, shown in the shaded regions of Figure 4.

The following comparisons utilized the peak maximum from the experimental spectra and detail our vibrational assignments based on the nearest predicted mode from the calculated spectra. With increasing chain length, the 1377 cm⁻¹ shift—a polymer peak, assigned to the coupled bending and stretching of the backbone carbons and first pendant carbon, increased relative to the CPP peak at 1452 cm⁻¹ shift, assigned to the bending of the hydrogens of the CPP propyl group. The same increase was seen comparing the 849 cm⁻¹ shift of pNAGA to the 887 cm⁻¹ shift of CPP, assigned to the amide carbon stretching, wagging of hydrogens on the primary amide, C-N-C bending of the secondary amide, and the C-C stretching of the CPP propyl group, respectively. A third example was observed in pNAGA₁₄₋₃₀ in the consistent decrease of the CPP

vibrations at 1282 and 1238 cm⁻¹ shift (assigned to the in-phase twisting of the hydrogens of the propyl group and the wagging of the same hydrogens, asymmetric stretch of S-C and C-C of chain side, respectively) relative to the 1199 cm⁻¹ shift peak of the pNAGA primary amide C-N-C asymmetric stretch and twisting of NH-CH₂ hydrogens. pNAGA₃₈ was excluded from this trend because the band at 1242 cm⁻¹ shift has the greatest magnitude of the triplet discussed. We hypothesize that this is due to the combined effect of the CPP vibrations already detailed at the location with a large amount of pNAGA character (wagging of NH-CH₂ hydrogrens, C-NH₂ stretch) as seen by the overlap of these peaks in calculated spectra (Figure 3). Because an increase in repeat unit character can be observed across the four pNAGA we can conclude that all chain lengths of pNAGA grafted to the surface are within the sensing volume of our SERS substrate. Thus, all polymers were determined to be valid, candidate affinity agents for AFB1 detection by SERS; all possessed multiple AFB1 interactions sites that were within the enhancing electromagnetic field.

The calculated normal Raman spectra of the monomer and anchoring group enabled the identification of pNAGA modes that may be affected by noncovalent binding of AFB1, specifically those of the repeat unit terminal amide. When used in conjunction with the experimental spectra of the four pNAGA molecular weights, the calculated spectra verified pNAGA attachment to the SERS substrate. The known modes of the calculated spectrum revealed spectral changes due to the increasing repeat unit character, relative to anchoring CTA group, with increasing chain length and demonstrated that the full chain resided within the enhancing electromagnetic field SERS substrate. This confirmed all pNAGA chain lengths as valid candidates for AFB1 SERS affinity agents.

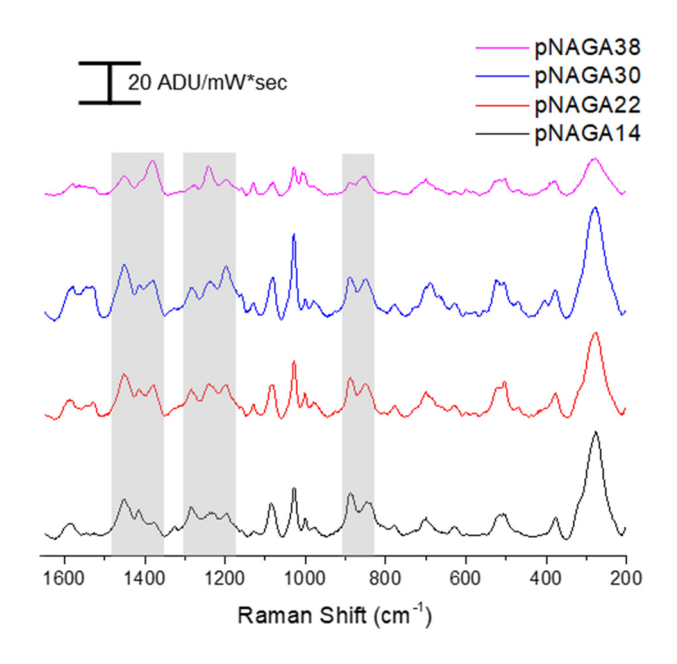


Figure 4. SERS of pNAGA polymers anchored to the FON substrates. Shaded regions identify polymer/CTA vibrations that change with increasing polymer length.

AFB1 Sensing with pNAGA-Functionalized FONS

Having confirmed the attachment of pNAGA to the FON SERS substrates and their inclusion in the sensing volume, pNAGA-functionalized FONS were exposed to 50 ppm AFB1 for 6 h in a 40% methanol aqueous solution. The averaged SERS spectra of the exposed FONs after a 1 mL water rinse is seen in Figure 5. The spectra of pNAGA₁₄ and pNAGA₃₈ FONs exposed to AFB1 (Figure 5A and 5D, respectively) showed no major differences from the polymer only spectra. We hypothesize that this is a result of polymer chain conformation on the FONs and the subsequent availability of NAGA repeat units for AFB1 noncovalent binding. Sterically, tightly packed chains would prohibit AFB1 access to mid-chain repeat units. pNAGA₁₄, which demonstrated adequate binding by ITC, is the shortest polymer tested and thus the self-assembly of it on the FON surface should be the densest. Dense packing of the polymer chains may facilitate intermolecular interactions among pNAGA, and decrease the number of

NAGA repeat units available for AFB1 interaction. The weak AFB1 binding to pNAGA₃₈ found in ITC was hypothesized to originate from the coiling of the polymer and intramolecular interactions. Similarly, at the FON surface, the grafted longest polymer can assume a random coil ('mushroom-like structure')⁶² with intramolecular hydrogen bonding, and expose fewer repeat units, decreasing AFB1 captured by the polymer layer. In addition, it is likely that any AFB1 associated with the pNAGA₃₈ is far from the most intense electromagnetic fields simply based on the size of the longest polymer length.

It is apparent from the SERS of 50 ppm AFB1 that there is an optimal length range of pNAGA for AFB1 SERS detection. pNAGA₂₂ and pNAGA₃₀ both display several spectral changes after AFB1 exposure (Figures 5B and 5C, respectively). There are large peak intensity increases at 600-628, 1195-1282, 1377, 1583 cm⁻¹ shift. All of these changes can be attributed, at least in part, to those pNAGA vibrations originating from the primary amide, predicted from the computational spectrum at 611, 1248, 1344, and 1561 cm⁻¹ shift. It is important to note that experimental AFB1 vibrations have been reported in these regions, specifically those from ring deformations at 624 cm⁻¹ shift, A(C–H₂)(C–H) (ring) at 1186 cm⁻¹ shift, β(C–H₂) (ring) at 1249 cm⁻¹ shift, β(C–H) ring deformation at 1274 cm⁻¹ shift, in plane CH₃ deformation at 1355 cm⁻¹ shift, and C-C and C-C-C stretching at 1592 cm⁻¹ shift.⁴¹ The colocalization of the pNAGA and AFB1 peaks makes it difficult to definitively assign the source of the new bands, though contributions from both were expected based on the proposed method of noncovalent binding hydrogen bonding between the primary amide of the repeat unit and the carbonyl and furan group of AFB1. Utilizing the strong performer pNAGA22-funtionalized FONs, lower AFB1 solutions were tested for SERS detection. Decreasing the concentration from 50 ppm AFB1 to 25 and 10 ppm (Figure S7 in Supporting Information) resulted in weak peak intensity changes and

high variance between FON replicates. Tethered to the FON surface, the pNAGA repeat units were not capturing sufficient AFB1 at lower solution concentrations to see strong intrinsic AFB1 signals or pNAGA signal changes.

pNAGA-functionalized FONs incubated with AFB1 demonstrated SERS spectral changes for those FONs decorated with optimal lengths of polymer: pNAGA₂₂ and pNAGA₃₀. FONs functionalized with short, densely-pack pNAGA₁₄ or long, intramolecularly associating pNAGA₃₈ appeared to be sterically hindered from capturing sufficient AFB1 to generate a change in signal. The spectral changes observed from FONs functionalized with pNAGA₂₂ and pNAGA₃₀ are in regions in which AFB1 vibrations are colocalized with pNAGA primary amide modes, and are likely the combination of both. These changes are not as prominent as the concentration is decreased from 50 ppm to 25 or 10 ppm. To be effective in the ppb AFB1 range, a modified strategy is needed for concentrating the AFB1 on the polymer chain and anchoring the chain to the SERS surface to maximize the signal of the pNAGA/AFB1 complex.

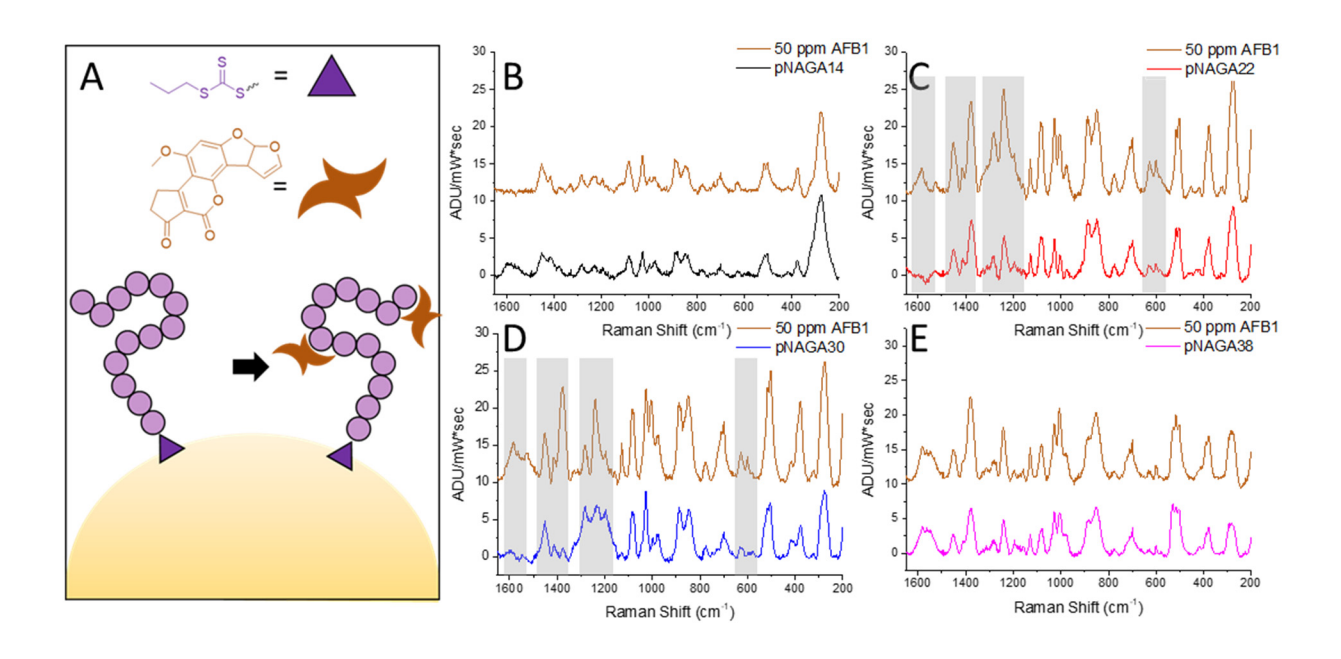


Figure 5. SERS from pNAGA-functionalized FONs exposed AFB1; (A) schematic representation of the exposure method (tethering of the polymer to the gold via the trithiocarbonate end group (purple triangle) followed by AFB1 exposure); (B-E) SERS from pNAGA only (bottom colored spectra) and pNAGA-FONS exposed to 50 ppm AFB1 (top brown spectra), shaded areas denote spectral changes observed that differed from the polymer alone.

AFB1 Sensing with pNAGA22/AFB1 Complex

To enable ppb detection of AFB1, we altered our order of attachment and exposure. Traditional SERS sensing experiments, such as those detailed above, first anchor affinity agents to the SERS substrate and subsequently exposed the functionalized substrate to the target. Below we detail experiments in which the pNAGA22 affinity agent was exposed in solution to AFB1 for 6 h and then attached to the FON for SERS sensing (Figure 6A). The long exposure of insolution pNAGA22 to AFB1 was proposed to form a polymer/toxin complex in solution, the whole of which would then be anchored to the FON through the trithiocarbonate of the pNAGA CTA. This new method was proposed to take full advantage of the benefits of a polymer affinity agent: all binding sites are free to assume the optimal conformation to noncovalently bind the maximum number of AFB1; binding sites near the CPP anchor can enable AFB1 localization in the highest enhancing region of the FON substrates. With more AFB1 molecules attached per chain and/or AFB1 molecules in higher enhancing fields, more signal was expected and lower AFB1 solution concentrations were probed. pNAGA₂₂ was used exclusively in these experiments as the polymer that maximized AFB1 binding in-solution, as shown by ITC, and at the surface, as shown by SERS from pNAGA-functionalized FONs.

Increasing AFB1 concentrations complexed with pNAGA₂₂ showed spectral changes relative to 0 ppm control experiment (Figure 6B). The spectral changes observed were similar to several changes seen in pNAGA-functionalized FONs exposed to 50 ppm AFB1. The two spectral changes that can be seen in all concentrations tested (as low as 10 ppb) was the increasing ratio of 1242 cm⁻¹ shift relative to the 1195 and 1279 cm⁻¹ shifts, and the increased magnitude at 1381 cm⁻¹shift. As previously stated, both the primary amide on pNAGA (1242 and 1377 cm⁻¹ shift) and AFB1 (1249 and 1355 cm⁻¹ shift), the proposed hydrogen bonding partners in the affinity agent/target complex, have strong modes in these regions.

The spectral change most dependent AFB1 concentration was found to be the peak height at 1380 cm⁻¹ shift, normalized by the CPP vibration at 688 cm⁻¹ shift (identified above from the calculated spectrum). Using a one-way ANOVA and Tukey post hoc analysis, this peak change was statistically significant as low at 100 ppb. This spectral feature, observed in the averages as low 10 ppb, was not significant at this lower concentration due to the high amount of variance between replicates. The source of this variance is hypothesized to result from high heterogenicity in the FON SERS substrates, which results in variance in the electromagnetic field, and thus spectra. Other peaks ratios were analyzed and were not statistically significant from one another.

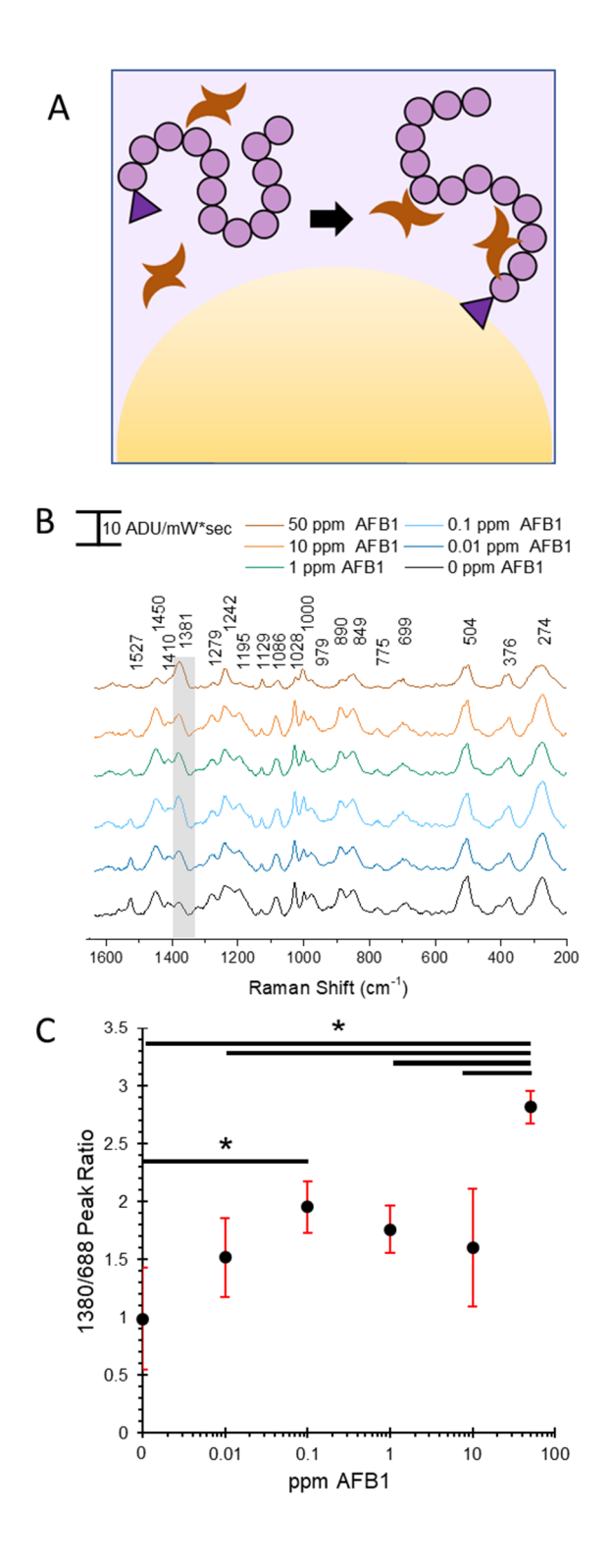


Figure 6. SERS from pNAGA₂₂/AFB1 complex assembled before immobilization on the SERS substrate; (A) schematic representation of the new exposure method (pre-exposure of the polymer containing a trithiocarbonate end group to AFB1 in solution and then tethering to the

gold), (B) spectra of the complex form from 0.01-50 ppm, and (C) the average 1380 cm^{-'1} shift peak intensity normalized by the 688 cm⁻¹ shift peak intensity, the negative control (0 ppm) has been added to this plot as a point of reference; error bars represent standard deviation, and * denotes statistically significant differences (p< 0.05).

The new method of complexing polymer and target prior to attachment to the SERS substrate improved the detection limit of the polymer-SERS platform. Using the same spectral changes identified in pNAGA-functionalized FONs exposed to AFB1, the pNAGA22/AFB1 complex was statistically different from the control at 100 ppb. This is a ten-fold improvement over bare FONs exposed to AFB1, an improvement that may be even greater for targets that have poorer chemisorption to gold than AFB1. Freer molecular motion of the pNAGA22 during exposure to AFB1 enabled improved noncovalent binding that resulted in higher SERS signal.

Reduction of the pNAGA Trithiocarbonate End Group

The improved SERS detection of AFB1, enabled by in-solution interaction with pNAGA₂₂, relies on tracking spectral regions that include vibrations from the trithiocarbonate moiety of the pNAGA CTA group, the NAGA repeat units, and AFB1. Specifically, the pNAGA₂₂, as synthesized by RAFT, demonstrates strong trithiocarbonate vibrations at 1451 cm⁻¹ shift (CH₃-CH₂ H bending), 1242 cm⁻¹ shift (C=S and CH₂-CH₂ asymmetric stretch), 1195 cm⁻¹ shift (CH₃-CH₂-CH₂ H rocking/twisting), 1028 cm⁻¹ shift (C=S and C-C symmetric stretch), 888 cm⁻¹ shift (CH₃-CH₂-CH₂ C-C symmetric stretch), 688 cm⁻¹ shift (S-C stretch), and 503 cm⁻¹ shift (symmetric 'breathing' of CS₂=S bonds). Our computational assignments of C=S vibrations are confirmed by literature, a strong C=S stretching mode can be observed anywhere from 1020 – 1250 cm⁻¹.63,64 These pNAGA CTA vibrational modes were hypothesized to be masking AFB1

vibrational modes of interest, and thus, modifying this end group to a thiol was undertaken to decrease the number of pNAGA vibrational modes and potentially increase AFB1 signal. Using *N*-propylamine and tris(2-carboxyethyl) phosphine HCl (TCEP), the trithiocarbonate end group was reduced to a thiol group. The majority of CTA reduction in polymer literature is done to further modify the chain end. With thiol endgroups, coupling between the reactive thiols, resulting in disulfide species, was expected.⁸ This was not seen as a disadvantage as disulfide coupled chains have been previously reported to bind more strongly to gold surfaces than polymers with a terminal sulfur moiety, an effect that is hypothesized to originate from cleavage of the S-S bond at the gold surface to yield a S-Au bond.⁵⁰ Modification of the end group was characterized by comparison of the pNAGA₂₂ SERS before and after reduction (Figure S9 in Supporting Information). Decreased magnitude at CTA vibrations detailed above (1451, 1242, 1195, 1028, 888, 688, and 503 cm⁻¹ shift) were observed, resulting in a pNAGA₂₂-SH spectrum with fewer peaks.

The pNAGA₂₂-SH was used to functionalize FONs, and the polymer-decorated substrates were exposed to 50 ppm AFB1 for 6 hrs (Figure 7A). The FONs exposed to AFB1 showed six new features not seen in the solvent control (Figure 7B). These features, seen at 1616, 1482, 1302, 819, 674, 626 cm¹ shift, are new peak shoulders and peaks shifts. Although all the features are small in magnitude, they correspond well with AFB1 vibrational modes previously reported in the literature at 1620, 1491, 1303, 813, 686, and 624 cm⁻¹ shift.⁴¹ The magnitude of these features was below an acceptable signal/noise ratio, and two rationales were proposed: the low stoichiometric ratio of AFB1 relative to the polymer chains resulted in less signal or capture of the AFB1 on the top of a dense pNAGA₂₂-SH layer held the AFB1 in a less enhancing region of the electromagnetic field of the FON, leading to less signal. Slavin *et al.* previously observed

more mass adsorbed on gold from disulfide polymers compared to other sulfur-containing species, and suggested the disulfides aligned on a planar axis to gold. Supported by this literature evidence, the argument for dense pNAGA22-SH FON coverage resulting in low AFB1 signals was accepted. It was hypothesized that using the method of first complexing polymer/AFB1 prior to substrate attachment, as detailed above for pNAGA22-CTA, would improve the detection of AFB1 by SERS enabled by pNAGA22-SH. Experimental spectra of CTA-only FON and SH-only FON can be seen in the Supporting Information (S10).

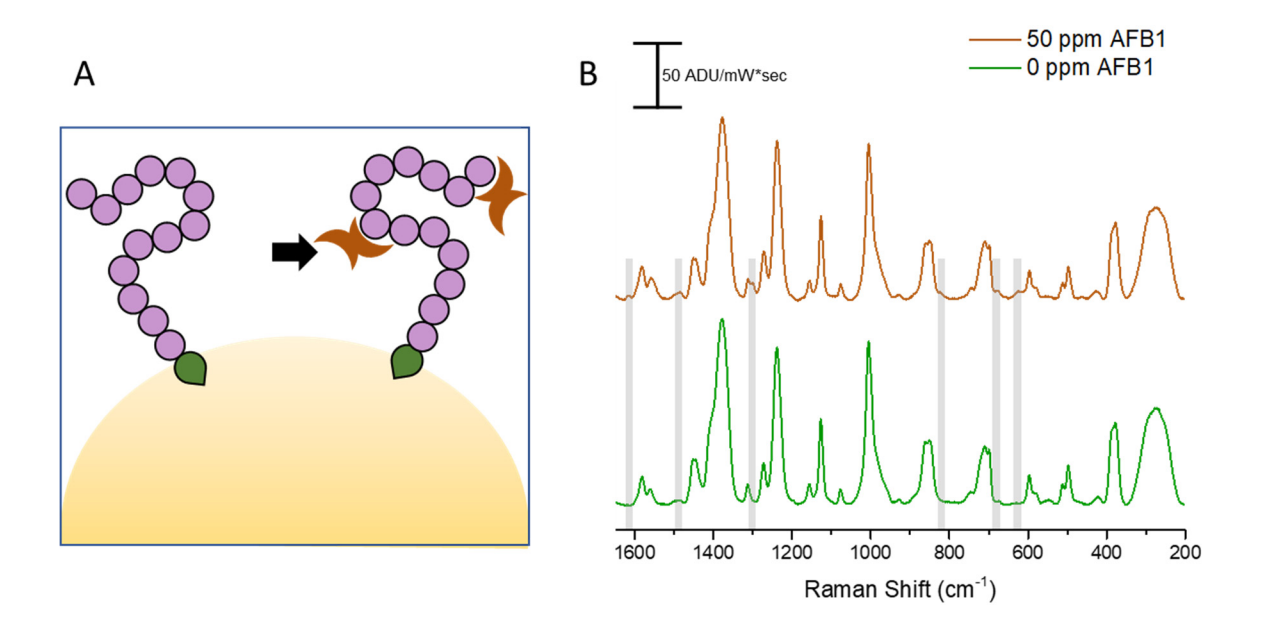


Figure 7. SERS from pNAGA₂₂-SH -functionalized FONs exposed to AFB1. (A) schematic representation of the exposure method (tethering of the polymer to the gold via the thiol end group (green teardrop) followed by AFB1 exposure); (B) SERS from pNAGA₂₂-SH only (bottom green spectrum) and pNAGA₂₂-SH-FONS exposed to 50 ppm AFB1 (top brown spectrum), shaded areas denote spectral changes observed that differed from the polymer alone and correlate with previously reported AFB1 peaks.⁴¹

A final attachment/affinity/sensing scheme was explored; pNAGA22-SH was complexed with varying concentrations of AFB1 and then grafted onto the FON surface (Figure 8A). The SERS, normalized to the 702 cm⁻¹ shift peak height, can be seen in Figure 8B. Fewer spectral changes due to AFB1 were identified using this method. The most notable is a growing shoulder at 712 cm⁻¹ shift. The nearest assigned modes from pNAGA and AFB1 are a CH-C symmetric stretch, with small contributions from NH-CH₂-C bending, calculated at 736 cm⁻¹ shift and C-H in-plane bending seen experimentally for AFB1 at 686 cm⁻¹ shift, 41 respectively. Because these NAGA and AFB1 vibrations are not very near the observed change, we hypothesize the change seen at 702 cm⁻¹ shift is due to a change in the S-C stretch of the thiol upon AFB1 incubation. In all concentrations tested (0.01, 0.1, 1, 10, and 50 ppm), the 712/702 cm⁻¹ shift ratio was statistically different from the AFB1-free solvent control. Most notably, complexing pNAGA22-SH and AFB1 prior to SERS detection led to the lowest statistical discernment of AFB1 from the control (10 ppb). The US FDA regulatory limit for AFB1 is 20 ppb; indeed, this result clearly demonstrates the potential of our platform for relevant AFB1 detection. Yet, the platform did not provide multiple unique, assignable vibrations of AFB1, a usual feature for a SERS sensor that would be used to detect multiple analytes from complex samples. The degree of pNAGA22-SH character in the spectra and weaker binding in solution are potential reasons for the lack of multiple spectral features. If pNAGA22-SH exists as coupled disulfide chains in solution, based on the ITC results detailed above, we predict the coupled chains would have poor in-solution AFB1 binding due to an effective chain length of 44 repeat units. Future work will explore very short oligomeric pNAGA-SH, <11 repeat units, to create a SERS sensing platform using the polymer/AFB1 complexation method. We hypothesize this would optimize in-solution

complexation of AFB1 and decrease the pNAGA character in the spectrum, potentially leading to the visualization of multiple unique, assignable vibrations of AFB1.

Reduction of the trithiocarbonate end group on pNAGA22 to a thiol was clear comparing the two SERS spectra. Vibrations assigned to the CPP disappeared, resulting in a simplified spectrum for pNAGA22-SH. Functionalizing FONs with this polymer and exposing the platform to 50 ppm AFB1, numerous small vibrations attributable to AFB1 were observed. To obtain AFB1 detection at lower concentrations, larger signal is needed. This was achieved complexing AFB1 and pNAGA22-SH prior to attachment to the FON. Using this method and analyzing the ratio of 712/702 cm⁻¹ shift, AFB1 concentrations 0.01, 0.1, 1, 10, and 50 ppm were found statistically different from the control. The lowest concentration is below the US FDA regulatory limit through further work with shorter pNAGA-SH is suggested to generate multiple unique, assignable vibrations of AFB1. The suggested improvement would enable detection and differentiation of multiple analytes and, thus, make the platform more commercially viable.

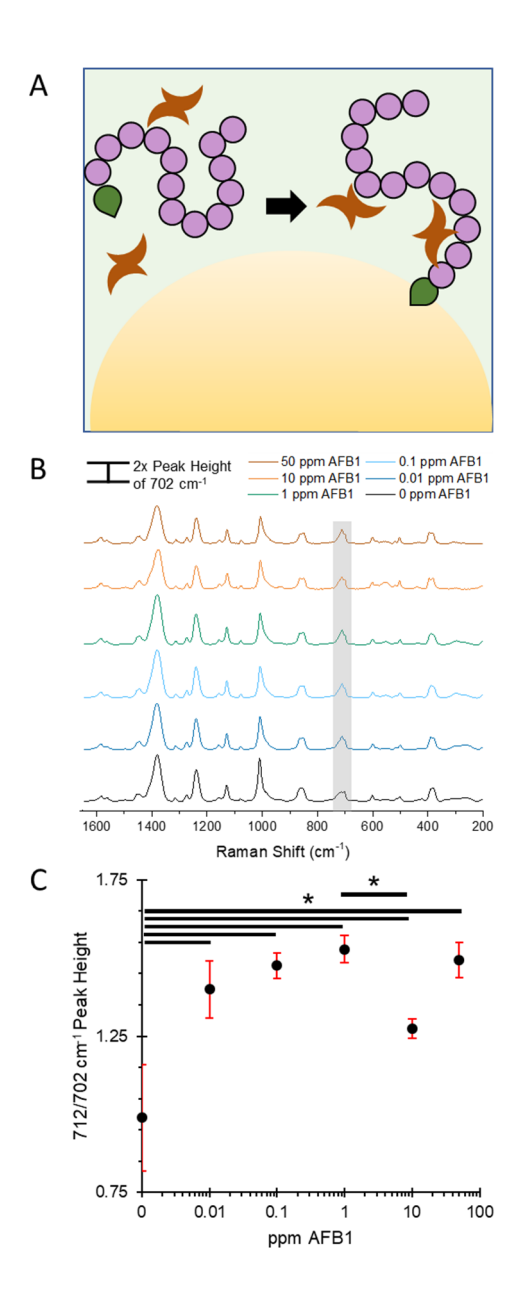


Figure 8. SERS from pNAGA22-SH/AFB1 complex assembled ahead of immobilization on the SERS substrate; (A) schematic representation of the exposure method (pre-exposure of the polymer containing the thiol end group to AFB1 and then tethering to the gold), (B) 702 cm⁻¹ shift normalized spectra of the complex form from 0.01-50 ppm, (C) the average 712 cm⁻¹ shift height normalized by 702 cm⁻¹ shift, the negative control (0 ppm) has been added to this plot as a

point of reference; error bars represent standard deviation and * denote statistical significance (p<0.05).

CONCLUSIONS:

Herein, polymer features were explored that can be tuned to optimize their use as affinity agents in sensing platforms. Starting from a monomer (NAGA) with hypothesized affinity for the biotoxin AFB1, and targeting SERS as a signal transduction mechanism, four polymers with distinct molecular weights were created by RAFT. These polymers were used to explore the role of molecular weight, anchoring chemistry, and order of addition (pre- or post- functionalization of the substrate) on the sensitivity of AFB1 detection. From our results, we posit four means by which polymer properties can influence performance as an affinity agent on a sensing platform: (i) In-solution, noncovalent binding between polymer and target is a function of the polymer chain conformation due to a decreased number of available binding sites on polymers engaged in intramolecular interactions; our ITC results demonstrated shorter pNAGA polymers such as pNAGA₁₄ and pNAGA₂₂ performed better in solution than their longer counterparts, pNAGA₃₀ and pNAGA₃₈. (ii) Polymer surface packing and conformation (extended or coiled chain) can sterically hinder the polymer/target binding at the surface; pNAGA22 and pNAGA30funtionalized SERS substrates exposed to 50 ppm AFB1 demonstrated the most AFB1 signal, while no AFB1 SERS signal was seen from the shortest and longest pNAGA samples. (iii) The freer molecular conformation of the untethered polymer in-solution enables improved target binding; complexing pNAGA22 and AFB1 prior to SERS substrate attachment improved the detection limit of the polymer-SERS platform; the pNAGA₂₂/AFB1 complex was statistically different from the control at 100 ppb AFB1. (iv) Altering the polymer attachment chemistry to decrease interference with the transduction mechanism of the sensor can significantly improve

platform sensitivity; reduction of the trithiocarbonate to a thiol simplified the pNAGA₂₂-SH

spectrum and complexing AFB1 and pNAGA22-SH prior to SERS substrate attachment enabled

detection of 10 ppb AFB1.

The lowest concentration of AFB1 detected by the pNAGA-SH enabled SERS platform

is below the US FDA regulatory limit of 20 ppb. Our thorough study of how molecular weight

and anchoring chemistry affect AFB1 capture, and SERS detection, can inform the design of

future sensing platforms targeting other analyte species. Based on our results, future work to

detect AFB1 should use a pNAGA-SH <11 repeat units to have excellent in-solution capture of

AFB1, and a simplified, lower magnitude pNAGA-SH signal that should enable the detection of

multiple unique, assignable vibrations of AFB1. Such a platform would enable detection and

differentiation of multiple analytes and, thus, make a very commercially viable platform.

ASSOCIATED CONTENT

Supporting Information. The Supporting Information (SI) 3The Supporting Information is

available free of charge on the ACS Publications website.

AUTHOR INFORMATION

Corresponding Author

*E-mail: chaynes@umn.edu Phone (work): 612-626-1096. Fax: 612-626-7541.

*Email: treineke@umn.edu Phone (work): 612-624-8042, Fax: 612-626-7541.

Author Contributions

32

The manuscript was written through contributions of all authors. All authors have given approval to the final version of the manuscript. ‡These authors contributed equally.

ACKNOWLEDGMENT

Isothermal titration calorimetry was carried out using an ITC-200 microcalorimeter, funded by the NIH Shared Instrumentation Grant S10-OD017982. We would like to acknowledge 3M for their collaboration and funding. MB and GCS were supported by NSF Grant CHE-1760537

REFERENCES

- (1) Carvalho, W. S. P.; Wei, M.; Ikpo, N.; Gao, Y.; Serpe, M. J. Polymer-Based Technologies for Sensing Applications. *Anal. Chem.* **2018**, *90* (1), 459–479.
- (2) Hydrogels in Sensing Applications. *Prog. Polym. Sci.* **2012**, *37* (12), 1678–1719.
- (3) Electrochemical Sensors and Biosensors Based on Redox Polymer/Carbon Nanotube Modified Electrodes: A Review. *Anal. Chim. Acta* **2015**, *881*, 1–23.
- (4) Molecularly-Imprinted Polymer Sensors: Realising Their Potential. *Biosens. Bioelectron.* **2016**, *76*, 131–144.
- (5) Ting, J. M.; Tale, S.; Purchel, A. A.; Jones, S. D.; Widanapathirana, L.; Tolstyka, Z. P.; Guo, L.; Guillaudeu, S. J.; Bates, F. S.; Reineke, T. M. High-Throughput Excipient Discovery Enables Oral Delivery of Poorly Soluble Pharmaceuticals. *ACS Cent. Sci.* **2016**, 2 (10), 748–755.
- (6) Hawker, C. J.; Wooley, K. L. The Convergence of Synthetic Organic and Polymer Chemistries. *Science* **2005**, *309* (5738), 1200–1205.
- (7) Gauthier, M. A.; Gibson, M. I.; Klok, H.-A. Synthesis of Functional Polymers by Post-Polymerization Modification. *Angew. Chem. Int. Ed.* **2009**, *48* (1), 48–58.
- (8) Willcock, H.; K. O'Reilly, R. End Group Removal and Modification of RAFT Polymers. *Polym. Chem.* **2010**, *1* (2), 149–157.
- (9) Braunecker, W. A.; Matyjaszewski, K. Controlled/Living Radical Polymerization: Features, Developments, and Perspectives. *Prog. Polym. Sci.* **2007**, *32* (1), 93–146.
- (10) Chen, L.; Xu, S.; Li, J. Recent Advances in Molecular Imprinting Technology: Current Status, Challenges and Highlighted Applications. *Chem. Soc. Rev.* **2011**, *40* (5), 2922–2942.
- (11) Vermeer, A. W.; Norde, W. The Thermal Stability of Immunoglobulin: Unfolding and Aggregation of a Multi-Domain Protein. *Biophys. J.* **2000**, 78 (1), 394–404.
- (12) Porta, A. L.; Sánchez-Iglesias, A.; Altantzis, T.; Bals, S.; Grzelczak, M.; Liz-Marzán, L. M. Multifunctional Self-Assembled Composite Colloids and Their Application to SERS Detection. *Nanoscale* **2015**, *7* (23), 10377–10381.
- (13) Pal, A.; Stokes, D. L.; Alarie, J. P.; Vo-Dinh, T. Selective Surface-Enhanced Raman Spectroscopy Using a Polymer-Coated Substrate. *Anal. Chem.* **1995**, *67* (18), 3154–3159.

- (14) Qian, C.; Guo, Q.; Xu, M.; Yuan, Y.; Yao, J. Improving the SERS Detection Sensitivity of Aromatic Molecules by a PDMS-Coated Au Nanoparticle Monolayer Film. *RSC Adv.* **2015**, *5* (66), 53306–53312.
- (15) Mueller, M.; Tebbe, M.; Andreeva, D. V.; Karg, M.; Alvarez Puebla, R. A.; Pazos Perez, N.; Fery, A. Large-Area Organization of PNIPAM-Coated Nanostars as SERS Platforms for Polycyclic Aromatic Hydrocarbons Sensing in Gas Phase. *Langmuir* 2012, 28 (24), 9168–9173.
- (16) Vo-Dinh, T.; Stokes, D. L. Surface-Enhanced Raman Detection of Chemical Vapors with the Use of Personal Dosimeters. *Field Anal. Chem. Technol.* **1999**, *3* (6), 346–356.
- (17) Haynes, C. L.; McFarland, A. D.; Duyne, R. P. V. Surface-Enhanced Raman Spectroscopy. *Anal. Chem.* **2005**, *77* (17), 338 A–346 A.
- (18) Haynes, C. L.; Yonzon, C. R.; Zhang, X.; Van Duyne, R. P. Surface-Enhanced Raman Sensors: Early History and the Development of Sensors for Quantitative Biowarfare Agent and Glucose Detection. *J. Raman Spectrosc.* **2005**, *36* (6–7), 471–484.
- (19) Bantz, K. C.; Meyer, A. F.; Wittenberg, N. J.; Im, H.; Kurtuluş, Ö.; Lee, S. H.; Lindquist, N. C.; Oh, S.-H.; Haynes, C. L. Recent Progress in SERS Biosensing. *Phys. Chem. Chem. Phys. PCCP* **2011**, *13* (24), 11551–11567.
- (20) Fenske, M. R.; Braun, W. G.; Wiegand, R. V.; Quiggle, D.; McCormick, R. H.; Rank, D. H. Raman Spectra of Hydrocarbons. *Anal. Chem.* **1947**, *19* (10), 700–765.
- (21) Raman, C. V.; Krishnan, K. S. A New Type of Secondary Radiation. *Nature* **1928**, *121* (3048), 501.
- (22) Beumers, P.; Brands, T.; Koss, H.-J.; Bardow, A. Model-Free Calibration of Raman Measurements of Reactive Systems: Application to Monoethanolamine/Water/CO2. *Fluid Phase Equilibria* **2016**, *424*, 52–57.
- (23) Chinnakkannu Vijayakumar, S.; Venkatakrishnan, K.; Tan, B. SERS Active Nanobiosensor Functionalized by Self-Assembled 3D Nickel Nanonetworks for Glutathione Detection. *ACS Appl. Mater. Interfaces* **2017**, *9* (6), 5077–5091.
- (24) Mayer, K. M.; Hafner, J. H. Localized Surface Plasmon Resonance Sensors. *Chem. Rev.* **2011**, *111* (6), 3828–3857.
- (25) Le Ru, E. C.; Blackie, E.; Meyer, M.; Etchegoin, P. G. Surface Enhanced Raman Scattering Enhancement Factors: A Comprehensive Study. *J. Phys. Chem. C* **2007**, *111* (37), 13794–13803.
- (26) He, L.; Deen, B.; Rodda, T.; Ronningen, I.; Blasius, T.; Haynes, C.; Diez-Gonzalez, F.; Labuza, T. P. Rapid Detection of Ricin in Milk Using Immunomagnetic Separation Combined with Surface-Enhanced Raman Spectroscopy. *J. Food Sci.* **2011**, *76* (5), N49–N53.
- (27) Ko, J.; Lee, C.; Choo, J. Highly Sensitive SERS-Based Immunoassay of Aflatoxin B1 Using Silica-Encapsulated Hollow Gold Nanoparticles. *J. Hazard. Mater.* **2015**, *285*, 11–17.
- (28) Wang, Z.; Zong, S.; Wu, L.; Zhu, D.; Cui, Y. SERS-Activated Platforms for Immunoassay: Probes, Encoding Methods, and Applications. *Chem. Rev.* **2017**, *117* (12), 7910–7963.
- (29) Campos, A. R.; Gao, Z.; Blaber, M. G.; Huang, R.; Schatz, G. C.; Van Duyne, R. P.; Haynes, C. L. Surface-Enhanced Raman Spectroscopy Detection of Ricin B Chain in Human Blood. *J. Phys. Chem. C* **2016**, *120* (37), 20961–20969.

- (30) He, L.; Lamont, E.; Veeregowda, B.; Sreevatsan, S.; Haynes, C. L.; Diez-Gonzalez, F.; Labuza, T. P. Aptamer-Based Surface-Enhanced Raman Scattering Detection of Ricin in Liquid Foods. *Chem. Sci.* **2011**, *2* (8), 1579.
- (31) Negri, P.; Chen, G.; Kage, A.; Nitsche, A.; Naumann, D.; Xu, B.; Dluhy, R. A. Direct Optical Detection of Viral Nucleoprotein Binding to an Anti-Influenza Aptamer. *Anal. Chem.* **2012**, *84* (13), 5501–5508.
- (32) Zhao, Y.; Yang, Y.; Luo, Y.; Yang, X.; Li, M.; Song, Q. Double Detection of Mycotoxins Based on SERS Labels Embedded Ag@Au Core-Shell Nanoparticles. *ACS Appl. Mater. Interfaces* **2015**, *7* (39), 21780–21786.
- (33) Gao, W.; Li, B.; Yao, R.; Li, Z.; Wang, X.; Dong, X.; Qu, H.; Li, Q.; Li, N.; Chi, H.; et al. Intuitive Label-Free SERS Detection of Bacteria Using Aptamer-Based in Situ Silver Nanoparticles Synthesis. *Anal. Chem.* **2017**, *89* (18), 9836–9842.
- (34) Szlag, V. M.; Styles, M. J.; Madison, L. R.; Campos, A. R.; Wagh, B.; Sprouse, D.; Schatz, G. C.; Reineke, T. M.; Haynes, C. L. SERS Detection of Ricin B-Chain via N-Acetyl-Galactosamine Glycopolymers. *ACS Sens.* **2016**, *1* (7), 842–846.
- (35) Duy, T. N.; Lam, P. K. S.; Shaw, G. R.; Connell, D. W. Toxicology and Risk Assessment of Freshwater Cyanobacterial (Blue-Green Algal) Toxins in Water. In *Reviews of Environmental Contamination and Toxicology*; Reviews of Environmental Contamination and Toxicology; Springer, New York, NY, 2000; pp 113–185.
- (36) Hussein, H. S.; Brasel, J. M. Toxicity, Metabolism, and Impact of Mycotoxins on Humans and Animals. *Toxicology* **2001**, *167* (2), 101–134.
- (37) Eaton, D. L.; Groopman, J. D. *The Toxicology of Aflatoxins: Human Health, Veterinary, and Agricultural Significance*; Elsevier, 2013.
- (38) Center for Food Safety and Applied Nutrition. Chemical Contaminants, Metals, Natural Toxins & Pesticides Guidance for Industry: Action Levels for Poisonous or Deleterious Substances in Human Food and Animal Feed http://www.fda.gov/Food/GuidanceRegulation/GuidanceDocumentsRegulatoryInformatio n/ChemicalContaminantsMetalsNaturalToxinsPesticides/ucm077969.htm#afla (accessed Jun 10, 2016).
- (39) The Grain Inspection, Packers and Stockyards Administration. GIPSA's Role in Aflatoxin Testing https://www.gipsa.usda.gov/fgis/aflatoxin.aspx (accessed Jan 22, 2018).
- (40) Lee, K.-M.; Herrman, T. J.; Bisrat, Y.; Murray, S. C. Feasibility of Surface-Enhanced Raman Spectroscopy for Rapid Detection of Aflatoxins in Maize. *J. Agric. Food Chem.* **2014**, *62* (19), 4466–4474.
- (41) Wu, X.; Gao, S.; Wang, J.-S.; Wang, H.; Huang, Y.-W.; Zhao, Y. The Surface-Enhanced Raman Spectra of Aflatoxins: Spectral Analysis, Density Functional Theory Calculation, Detection and Differentiation. *Analyst* **2012**, *137* (18), 4226–4234.
- (42) Stuart, D. A.; Yuen, J. M.; Shah, N.; Lyandres, O.; Yonzon, C. R.; Glucksberg, M. R.; Walsh, J. T.; Van Duyne, R. P. In Vivo Glucose Measurement by Surface-Enhanced Raman Spectroscopy. *Anal. Chem.* **2006**, *78* (20), 7211–7215.
- (43) Kim, D.; Campos, A. R.; Datt, A.; Gao, Z.; Rycenga, M.; Burrows, N. D.; Greeneltch, N. G.; Mirkin, C. A.; Murphy, C. J.; Duyne, R. P. V.; et al. Microfluidic-SERS Devices for One Shot Limit-of-Detection. *Analyst* 2014, 139 (13), 3227–3234.
- (44) Zaleski, S.; Clark, K. A.; Smith, M. M.; Eilert, J. Y.; Doty, M.; Van Duyne, R. P. Identification and Quantification of Intravenous Therapy Drugs Using Normal Raman

- Spectroscopy and Electrochemical Surface-Enhanced Raman Spectroscopy. *Anal. Chem.* **2017**, *89* (4), 2497–2504.
- (45) Haynes, C. L.; Van Duyne, R. P. Nanosphere Lithography: A Versatile Nanofabrication Tool for Studies of Size-Dependent Nanoparticle Optics. *J. Phys. Chem. B* **2001**, *105* (24), 5599–5611.
- (46) Piletska, E.; Karim, K.; Coker, R.; Piletsky, S. Development of the Custom Polymeric Materials Specific for Aflatoxin B1 and Ochratoxin A for Application with the ToxiQuant T1 Sensor Tool. *J. Chromatogr. A* **2010**, *1217* (16), 2543–2547.
- (47) Szlag, V. M.; Jung, S.; Rodriguez, R.; Bryson, S.; Bourgeois, M.; Schatz, G. C.; Reineke, T. M.; Haynes, C. L. Isothermal Titration Calorimetry for the Screening of Aflatoxin B1 Surface-Enhanced Raman Scattering Sensor Affinity Agents. *Anal. Chem.* In Preparation.
- (48) Duwez, A.-S.; Guillet, P.; Colard, C.; Gohy, J.-F.; Fustin, C.-A. Dithioesters and Trithiocarbonates as Anchoring Groups for the "Grafting-To" Approach. *Macromolecules* **2006**, *39* (8), 2729–2731.
- (49) Fustin, C.-A.; Duwez, A.-S. Dithioesters and Trithiocarbonates Monolayers on Gold. *J. Electron Spectrosc. Relat. Phenom.* **2009**, *172* (1–3), 104–106.
- (50) Slavin, S.; Soeriyadi, A. H.; Voorhaar, L.; Whittaker, M. R.; Becer, C. R.; Boyer, C.; Davis, T. P.; Haddleton, D. M. Adsorption Behaviour of Sulfur Containing Polymers to Gold Surfaces Using QCM-D. *Soft Matter* **2011**, *8* (1), 118–128.
- (51) Ebeling, B.; Vana, P. RAFT-Polymers with Single and Multiple Trithiocarbonate Groups as Uniform Gold-Nanoparticle Coatings. *Macromolecules* **2013**, *46* (12), 4862–4871.
- (52) Zhou, C.; Hillmyer, M. A.; Lodge, T. P. Micellization and Micellar Aggregation of Poly(Ethylene-Alt-Propylene)-b-Poly(Ethylene Oxide)-b-Poly(N-Isopropylacrylamide) Triblock Terpolymers in Water. *Macromolecules* **2011**, *44* (6), 1635–1641.
- (53) Xu, X.; Smith, A. E.; Kirkland, S. E.; McCormick, C. L. Aqueous RAFT Synthesis of PH-Responsive Triblock Copolymer MPEO-PAPMA-PDPAEMA and Formation of Shell Cross-Linked Micelles†. *Macromolecules* **2008**, *41* (22), 8429–8435.
- (54) Seuring, J.; Bayer, F. M.; Huber, K.; Agarwal, S. Upper Critical Solution Temperature of Poly(N-Acryloyl Glycinamide) in Water: A Concealed Property. *Macromolecules* **2012**, 45 (1), 374–384.
- (55) Li, H.; Cortez, M. A.; Phillips, H. R.; Wu, Y.; Reineke, T. M. Poly(2-Deoxy-2-Methacrylamido Glucopyranose)-b-Poly(Methacrylate Amine)s: Optimization of Diblock Glycopolycations for Nucleic Acid Delivery. *ACS Macro Lett.* **2013**, *2* (3), 230–235.
- (56) te Velde, G.; Bickelhaupt, F. M.; Baerends, E. J.; Fonseca Guerra, C.; van Gisbergen, S. J. A.; Snijders, J. G.; Ziegler, T. Chemistry with ADF. *J. Comput. Chem.* **2001**, *22* (9), 931–967.
- (57) Becke, A. D. Density-Functional Exchange-Energy Approximation with Correct Asymptotic Behavior. *Phys. Rev. A* **1988**, *38* (6), 3098–3100.
- (58) Becke, A. D. A New Mixing of Hartree–Fock and Local Density-functional Theories. *J. Chem. Phys.* **1993**, *98* (2), 1372–1377.
- (59) R Core Team. R: A Language and Environment for Statistical Computing; R Foundation for Statistical Computing: Vienna, Austria, 2017.
- (60) Jung, S.; Lodge, T. P.; Reineke, T. M. Complexation between DNA and Hydrophilic-Cationic Diblock Copolymers. *J. Phys. Chem. B* **2017**, *121* (10), 2230–2243.

- (61) Du, X.; Li, Y.; Xia, Y.-L.; Ai, S.-M.; Liang, J.; Sang, P.; Ji, X.-L.; Liu, S.-Q. Insights into Protein–Ligand Interactions: Mechanisms, Models, and Methods. *Int. J. Mol. Sci.* **2016**, *17* (2), 144.
- (62) J.F. Douglas. Polymer Brushes: Structure and Dynamics. In *In Encyclopedia of Materials: Science and Technology*; Elsevier: New York, 2001; p 7218–7223.
- (63) Colthup, N. B.; Daly, L. H.; Wiberley, S. E. CHAPTER 12 COMPOUNDS CONTAINING BORON, SILICON, PHOSPHORUS, SULFUR, OR HALOGEN. In *Introduction to Infrared and Raman Spectroscopy (Second Edition)*; Academic Press, 1975; pp 335–364.
- (64) Blakey, I.; Schiller, T. L.; Merican, Z.; Fredericks, P. M. Interactions of Phenyldithioesters with Gold Nanoparticles (AuNPs): Implications for AuNP Functionalization and Molecular Barcoding of AuNP Assemblies. *Langmuir* **2010**, *26* (2), 692–701.

BRIEFS (Word Style "BH_Briefs"). If you are submitting your paper to a journal that requires a brief, provide a one-sentence synopsis for inclusion in the Table of Contents.

SYNOPSIS (Word Style "SN_Synopsis_TOC"). If you are submitting your paper to a journal that requires a synopsis, see the journal's Instructions for Authors for details.